A dominant vimentin mutant upregulates Hsp70 and the activity of the ubiquitin-proteasome system, and causes posterior cataracts in transgenic mice

Roland Bornheim[1,*,‡], Martin Müller[1,*], Uschi Reuter[1], Harald Herrmann[2], Heinrich Büssow[3] and Thomas M. Magin[1,§]

[1]Institut für Biochemie and Molekularbiologie, Abteilung für Zellbiochemie und LIMES, Universität Bonn, Nussallee 11, 53115 Bonn, Germany
[2]Department of Molecular Genetics, B065, German Cancer Research Center, 69120 Heidelberg, Germany
[3]Anatomisches Institut der Universität Bonn, Nussallee 10, 53115 Bonn, Germany

*These authors contributed equally to this work
‡Present address: Laboratory of Molecular Immunology, Program Unit Molecular Immune and Cell Biology, LIMES (Life and Medical Sciences Bonn), University of Bonn, 53115 Bonn, Germany
§Author for correspondence (e-mail: t.magin@uni-bonn.de)

Accepted 8 August 2008
Journal of Cell Science 121, 3737-3746 Published by The Company of Biologists 2008
doi:10.1242/jcs.030312

Summary

Vimentin is the main intermediate filament (IF) protein of mesenchymal cells and tissues. Unlike other IF$^{-/-}$ mice, vimentin$^{-/-}$ mice provided no evidence of an involvement of vimentin in the development of a specific disease. Therefore, we generated two transgenic mouse lines, one with a (R113C) point mutation in the IF-consensus motif in coil1A and one with the complete deletion of coil 2B of the rod domain. In epidermal keratins and desmin, point mutations in these parts of the α-helical rod domain cause keratinopathies and desminopathies, respectively. Here, we demonstrate that substoichiometric amounts of vimentin carrying the R113C point mutation disrupted the endogenous vimentin network in all tissues examined but caused a disease phenotype only in the eye lens, leading to a posterior cataract that was paralleled by the formation of extensive protein aggregates in lens fibre cells. Unexpectedly, central, postmitotic fibres became depleted of aggregates, indicating that they were actively removed. In line with an increase in misfolded proteins, the amounts of Hsp70 and ubiquitylated vimentin were increased, and proteasome activity was raised. We demonstrate here for the first time that the expression of mutated vimentin induces a protein-stress response that contributes to disease pathology in mice, and hypothesise that vimentin mutations cause cataracts in humans.

Supplementary material available online at
http://jcs.biologists.org/cgi/content/full/121/22/3737/DC1

Key words: Vimentin, Intermediate filaments, Dominant-negative mutation, Cataract formation, Protein misfolding, Chaperones, Proteasomes, Transgenic mice, Mouse model systems

Introduction

Vimentin is a type-III intermediate filament (IF) protein that has been highly conserved during vertebrate evolution. It displays a typical tripartite domain structure with a central α-helical rod-domain flanked by non-α-helical N- and C-terminal domains (Fig. 1A) (Herrmann and Aebi, 2004). In the mouse, vimentin expression starts at embryonic day 8.5 (E8.5) in primary mesenchymal cells that form the primitive streak (Franke et al., 1982). In adult mice, vimentin is present in all mesenchymal cells and tissues and, transiently, in the CNS and muscle (Bachmann et al., 1983; Colucci-Guyon et al., 1994). Altough vimentin can form homotypic IFs, it is frequently coexpressed and can heteropolymerise with desmin, synemin, nestin and GFAP (Robson et al., 2004; Granger and Lazarides, 1984; Michalczyk and Ziman, 2005).

In endothelial cells, vimentin interacts with several adhesion complexes (for a review, see Ivaska et al., 2007), namely α6β4-integrin-expressing focal adhesions through the linker protein plectin (Homan et al., 2002), as well as with α2β1- and αvβ3-integrin-positive focal adhesions (Kreis et al., 2005; Tsuruta and Jones, 2003). Synemin, itself an IF protein, can link type-III IF vimentin, desmin and GFAP to focal adhesions by interacting with talin and vinculin (Uyama et al., 2006). Vimentin has also been shown to interact directly with the small lens chaperone αB-crystallin (also known as CRYAB) (Djabali et al., 1997; Nicholl and Quinlan, 1994).

Among many established and recently discovered functions, the protection against mechanical stress and other forms of stress is a major function of IF proteins (for reviews, see Fuchs and Cleveland, 1998; Herrmann et al., 2007). To uncover these functions, gene-knockout and transgenic-mouse studies in which dominant keratin mutants were expressed proved most helpful to identify their role in various human diseases including epidermolysis bullosa simplex (EBS) and desmin myopathies (Magin et al., 2004; Magin et al., 2007; Omary et al., 2004; Bar et al., 2007 and references therein). In most settings, point mutations destroy the normal organisation of the cytoskeleton, and lead to the formation of cytoplasmic protein aggregates and extensive cell fragility in epidermis, heart and skeletal muscle, after the exposure to mechanical stress (Kim and Coulombe, 2007).

Protein aggregates that are typical for EBS, and resemble those found in other IF disorders and in many neurodegenerative diseases that are collectively referred to as protein-conformational disorders.

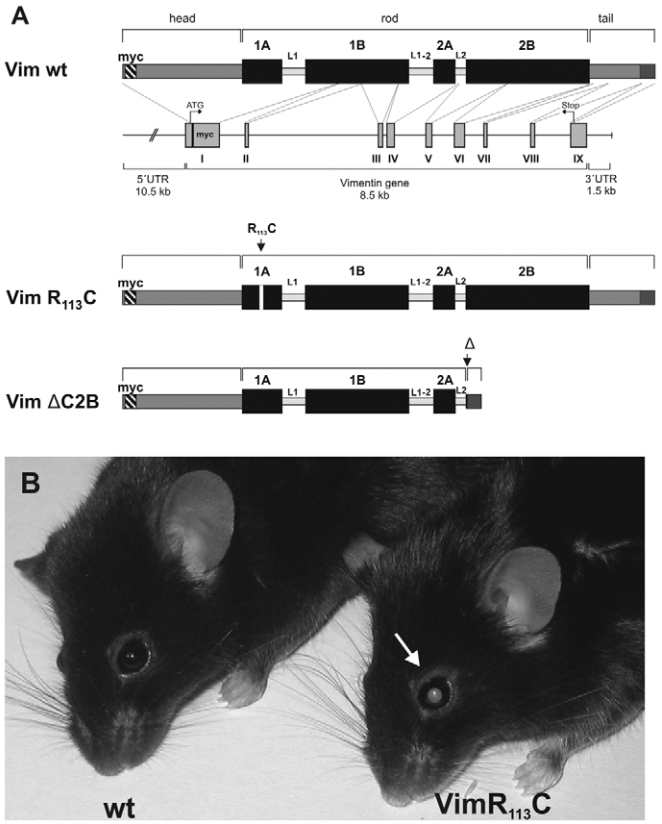

Fig. 1. Vimentin expression constructs and eye phenotype. (A) Schematic representation of the constructs used for expression of wildtype, $R_{113}C$ point-mutant ($VimR_{113}C$) and C-terminal truncated (VimΔC2B) vimentin transgene. All constructs are based on the mouse vimentin gene with its own regulatory elements. (B) Note turbid lens in a 22-week-old animal expressing the $VimR_{113}C$ mutant (arrow).

Although the corresponding pathomechanisms are not well understood, it is widely accepted that they result from a failure of different quality-control mechanisms for proteins. In addition to the accumulation of misfolded protein – which is specific for the disease – the common denominators of such protein aggregates are the presence of ubiquitin, components of the proteasome complex and molecular chaperones, including Hsp70 and Hsp40. Molecular chaperones assist the folding of nascent polypeptides, avoid the formation of protein aggregates and regulate the subcellular distribution of proteins to their correct localisation. Most importantly, chaperones facilitate either the refolding of mutant proteins or their removal by the protein degradation machinery. Hsp70 chaperones are able to bind a large number of non-native proteins in an ATP-dependent manner and are regulated by co-chaperones. Whereas the majority of co-chaperones serve the refolding of proteins into the native state, several co-chaperones that link chaperones to the ubiquitin-proteasome system have recently been identified (Arndt et al., 2007). The ubiquitin-proteasome system is responsible for the degradation of misfolded and short-lived proteins into peptide fragments (Arndt et al., 2007).

Despite extensive studies, solid information on specific functions of vimentin in different tissues and specific cell types in vivo is still limited. Most importantly, vimentin is one of the very few IF genes which so far has not been linked to a human disease (Magin et al., 2004; Magin et al., 2007; Kim and Coulombe, 2007). Based on the high degree of sequence conservation among vimentin and other IF proteins, such as desmins, we undertook a new approach to study the function of vimentin by expressing a mutated vimentin gene in mice. Many IF disorders are caused by mutations in coil 1A of the rod domain. The mutation R125C in the IF-consensus-sequence LNR in keratin K14 leads to the most severe form of EBS and induces an extensive collapse of the keratin cytoskeleton in humans and in transgenic mice (Fuchs and Cleveland, 1998). Given that the domain structure of IF proteins is highly conserved along the α-helical rod domain, we reasoned that an analogous mutation (R113C) in vimentin should have a strong impact on vimentin assembly and cytoskeletal architecture upon coexpression with the wild-type protein. Furthermore, we deleted the vimentin coil 2B domain, which according to analogous deletions in several other IF proteins, should completely collapse IF architecture (Albers and Fuchs, 1987; Rothnagel et al., 1999). We have recently shown that expression of the above vimentin variants in 3T3L1 fibroblasts disrupted the endogenous vimentin network and caused the formation of aggregates (Schietke et al., 2006). This rearrangement of the cytoskeleton was accompanied by an upregulation of the co-chaperones Hsp40 and Hsp25 and a decreased sensitivity to pro-apoptotic stimuli.

Here we report on two transgenic mouse lines, one in which a vimentin variant is expressed that carries the R113C point mutation ($VimR_{113}C$) and a second in which vimentin is expressed that lacks the entire coil2B domain (VimΔC2B). In both mouse lines, sub-stoichiometric amounts of mutant vimentin were sufficient to disrupt endogenous vimentin IF, without affecting the embryonic development and reproduction of transgenic mice. We discovered, however, the formation of a posterior cataract in the eye lens of adult mice, accompanied by the upregulation of Hsp70 and increased proteasome activity. The disappearance of vimentin aggregates in central lens fibres shows for the first time that IF aggregates are transient in vivo. Moreover, our data suggest that vimentin is a candidate gene involved in cataract formation.

Results

Age-dependent protein aggregation and cataract formation

We have previously demonstrated that the vimentin mutants $VimR_{113}C$ and VimΔC2B act dominant-negatively and prevent IF formation of wild-type vimentin during in vitro assembly in the test tube and in transfected cultured cells (Schietke et al., 2006). To analyse the consequences in vivo, transgenic mouse lines which express both vimentin mutants as Myc-tagged variants and a line expressing wild-type (wt) Myc-tagged vimentin serving as a control, were generated from founder animals expressing vimentin mutants at sub-stoichiometric levels (≤30%, see below) compared with endogenous vimentin (Fig. 1A; Fig. 3A). Except the results that demonstrate the formation of larger vimentin inclusions and a more-severe disruption of the lens capsule observed in VimΔC2B animals, all data described here were obtained in $VimR_{113}C$ mice. Morphological examination revealed turbid lenses and formation of cataracts in adult $VimR_{113}C$ but not in control animals (Fig. 1B). Subsequent histological examination on paraffin-embedded lenses indicated that those from $VimR_{113}C$ animals were far more fragile and displayed a disrupted fibre cell morphology (Fig. 2A-B').

As judged by immunofluorescence microscopy using anti-Myc and anti-vimentin antibodies, transgenic vimentin was expressed appropriately in all tissues examined, and predominantly formed cytoplasmic protein inclusions that also contained endogenous vimentin (data not shown). Despite extensive aggregation of the

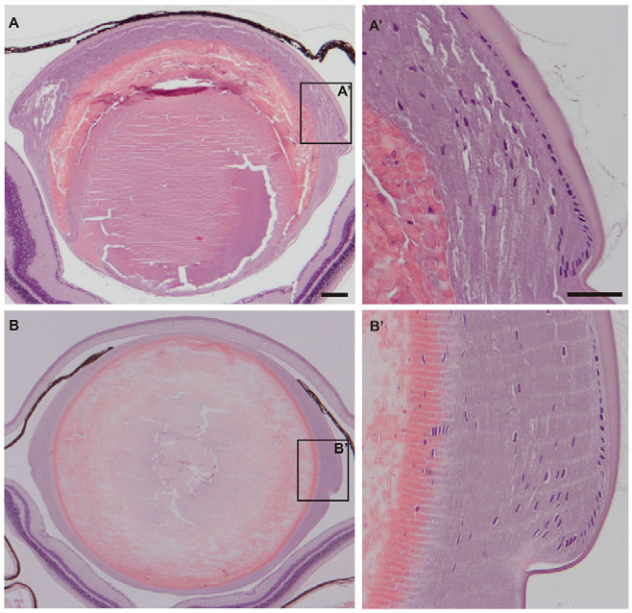

Fig. 2. Histology of eye of vimentin wildtype and VimR113C transgenic mice. (A,B) Haematoxylin and eosin (H&E) stained, paraffin-embedded lens sections of 45-week-old (A)VimR_{113}C transgenic and (B) wt mice. (A',B') Higher magnifications of the insets is shown in A and B. Note that VimR_{113}C lenses are much more fragile than wt lenses; they display a less regular organisation of fibre cells. Scale bars: 70 µm, (A,B), 60 µm (A',B').

vimentin cytoskeleton, all transgenic animals examined by us underwent normal embryonic development, showed no gross abnormalities and were fully fertile (data not shown). To identify the onset of cataract formation, we analysed animals at various stages of development by immunofluorescence microscopy, which revealed that protein aggregation was an age-dependent process. In lenses of newborn mice, VimR_{113}C colocalised to a large extent with endogenous vimentin but formed an apparently normal cytoskeleton (Fig. 3C), similar to the Myc-tagged wt vimentin serving as control (Fig. 3B). Large aggregates started around 6 weeks of age in lens fibre cells and became very prominent from twelve weeks onwards (Fig. 3E), whereas wt mice displayed a normal, submembraneous vimentin cytoskeleton (Fig. 3D).

To understand these observations at the molecular level, vimentin expression was quantified by immunoblotting soluble and insoluble lens proteins, in order to exclude that aggregation and catarcat formation were caused by overexpression of the transgenic protein. This revealed that VimR_{113}C represented ≤30% of endogenous vimentin in the eye lens and other tissues – a finding that is in agreement with cell culture studies and irrespective of the age of animals (Fig. 3A) (Schietke et al., 2006).

Altered membrane organisation and cell-context-dependent protein aggregation

To understand the basis of cataract formation, we performed electron microscopy (EM) on 11-week-old lenses of mutant and wt animals. Notably, vimentin aggregates were absent in the lens epithelium but began to accumulate immediately upon fibre cell differentiation. Aggregate formation upon expression of mutant vimentin was more severe in VimΔC2B mice. In VimR_{113}C and VimΔC2B mice, the plasma membrane of fibre cells was highly disorganised with multiple invaginations

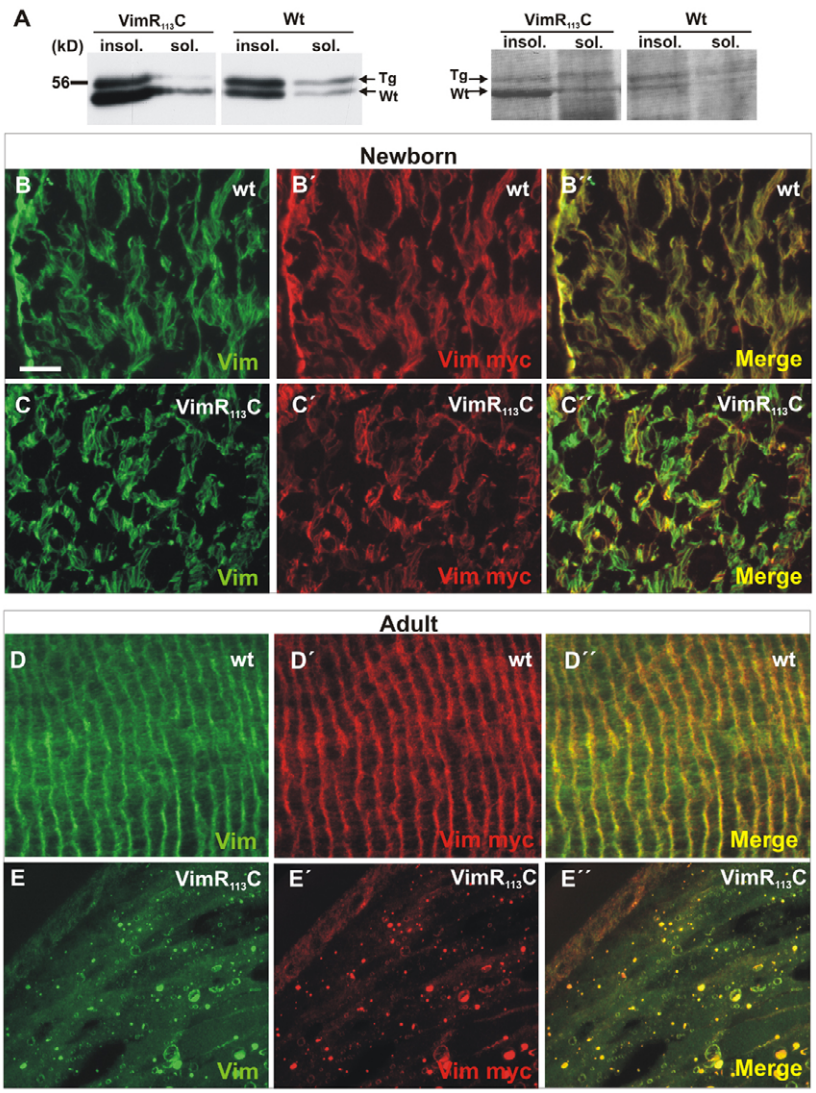

Fig. 3. Age-dependent aggregate and cataract formation. (A) Immunoblot analysis of endogenous and transgene vimentin in extracts of lenses from 4-month-old wt and VimR_{113}C mice. Endogenous and transgenic vimentin was detected using a vimentin antibody. Owing to the Myc-epitope present in the mutated vimentin, it migrates slower than endogenous vimentin. (B-E) Immunofluorescence analysis of lenses. Cryosections of newborn and 5-month-old animals were stained for total (green) and Myc-tagged vimentin (red). (B,D) Vimentin expression and localisation in the wt. (C,E) Vimentin expression in VimR_{113}C mice. In newborn mice, the distribution of VimR_{113}C protein is similar to wt vimentin but less homogenous. (E) Aggregate formation in fibre cells of adult animals. Note the high number and large size of vimentin aggregates in lenses from adult compared with those from new born animals (C',C'',E',E''). Bar: 20 µm.

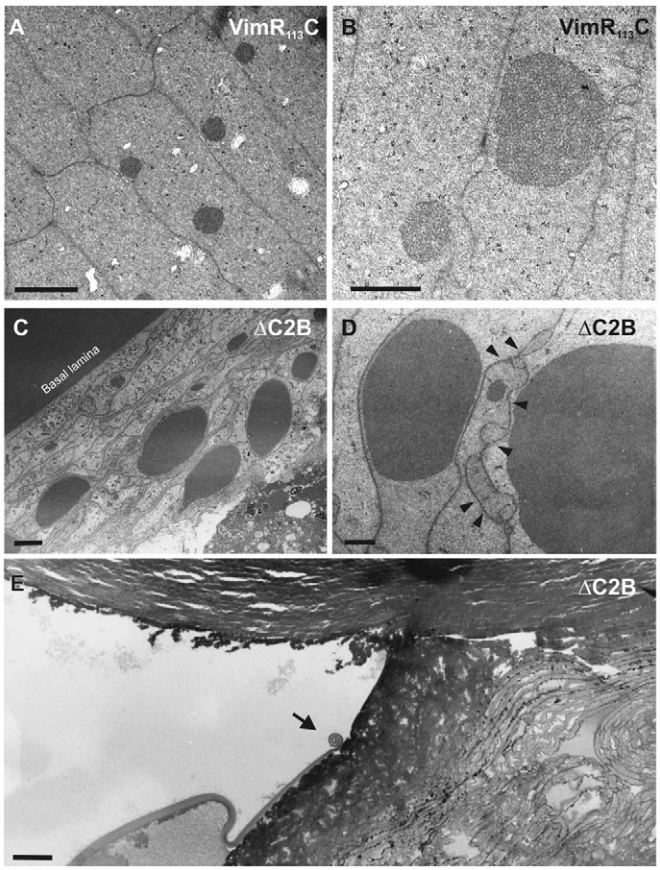

Fig. 4. Ultrastructure of lens fibre cells in mutant mice. (A,B) EM of vimentin aggregates in lens fibre cells of 11-week-old $VimR_{113}C$ mice. Vimentin aggregates appear amorphous with sharp boundaries and are not surrounded by membranes. At this stage, the plasma membrane is not yet strongly affected. (C,D) Notice the highly pleated organisation of the plasma membrane in VimΔC2B mice. (D) Vimentin aggregates and membrane reorganisation in VimΔC2B mice at high resolution. Aggregates are dense, different in size and not attached to or enclosed by a membrane. Arrowheads mark irregular membrane invaginations. (E) Semi-thin section of a lens from a 22-week-old VimΔC2B transgenic mouse. An arrow marks the disrupted basal lamina of the lens capsule. Lens fibres break through basal lamina and protrude into the vitreous body. Scale bars: 2 μm (A) 1 μm (B, D), 3 μm (C), 20 μm (E).

(Fig. 4D). This effect was not caused by a direct interaction of vimentin with lens-specific junctions and did not result from a disturbance of the membrane-attached actin and beaded-filament cytoskeleton (see Fig. 6) (Straub et al., 2003). EM furthermore revealed that aggregates were dense and not enclosed by a plasma membrane, excluding their incorporation into lysosomes (Fig. 4D). Ultimately, vimentin aggregation led to a posterior capsule rupture at the age of ~6 months, followed by protrusion of fibre cells into the posterior chamber. This phenotype was strongly reminiscent of the 'snowball cataract' described in humans (Fig. 4E) (Eshagian et al., 1981). The formation of a posterior cataract and disruption of lenses suggest that the mutated vimentin subunit represents a gain-of-function mutation.

Increased turnover of vimentin aggregates is accompanied by increased chaperone expression and proteasome activity

We have reported previously that protein aggregates that contain mutant keratins are highly dynamic structures with a half-life of less than 15 minutes in cultured cells (Werner et al., 2004). This observation prompted us to examine the size and distribution of vimentin aggregates in the lens. In contrast to the expectation that the aggregates should increase in size towards the centre of the lens – where the oldest, metabolically least active fibre cells are located – we discovered by confocal microscopy on frozen sections that they became smaller and finally disappeared (Fig. 5A-B). In the lens epithelium, aggregates were absent, as judged by EM (data not shown).

We hypothesised that, depending on the cellular context, $VimR_{113}C$ triggered a stress response. Misfolded proteins are known to induce molecular chaperones of the Hsp70 family. Furthermore, the small chaperone αB-crystallin is known to affect the organisation of vimentin (Nicholl and Quinlan, 1994; Perng et al., 1999). In lenses of $VimR_{113}C$ transgenic mice, we noticed a substantial upregulation of Hsp70, and most of the protein also colocalised with vimentin aggregates in addition to Hsp40 (supplementary material Fig. S1B' and S1A' for comparison; and data not shown) (Schietke et al., 2006). The increase in Hsp70 protein was also detectable in lens extracts of $VimR_{113}C$ compared with wt animals (Fig. 5E). It has been described previously that the upregulation of Hsp70 and the co-chaperone Hsp40 can be accompanied by an increased degradation of misfolded proteins via the proteasome (Brehmer et al., 2001). To examine this further, we investigated whether vimentin is poly-ubiquitylated in $VimR_{113}C$ lenses. Immunoprecipitation of extracts of total lens protein using a vimentin antibody followed by immunoblot analysis of ubiquitin revealed an increase of ubiquitylated vimentin in $VimR_{113}C$ (Fig. 5D). Next, we measured proteasome activity in transgenic fibre cells and in 3T3L1 fibroblasts stably transfected with $VimR_{113}C$. In both settings, proteasome activity was increased by ~30% compared with controls, suggesting that enhanced proteasome activity contributes to the removal of vimentin aggregates (Fig. 5C). During apoptosis, vimentin is a target for caspases 3, 6 and 7 (Byun et al., 2001). The analysis of caspase activity in extracts of lens tissue and of 3T3L1 cells stably transfected with $VimR_{113}C$ revealed no difference compared with wt controls (supplementary material Fig. S2A). Because caspase 3 and caspase 7 are key effectors of apoptosis, we furthermore conclude that lens pathology does not result from increased apoptosis. Finally, we addressed whether degradation of vimentin, a previously identified transglutaminase target in the lens, is impaired by crosslinking (Clement et al., 1998). Immunoblotting of lens proteins with a vimentin antibody revealed no evidence for crosslinked vimentin (supplementary material Fig. S2B).

Expression and organisation of CP49 and filensin remains unchanged

CP49 (also known as BFSP2) and filensin (also known as BFSP1), together with αB-crystallin form the so-called beaded filaments of the lens and are, based on gene knockout and human disease studies, essential for the structural integrity and optical capacity of the lens (Perng et al., 2007; Perng et al., 2004). In control lenses, filensin and vimentin displayed a similar distribution (Fig. 6A-A"). With regard to CP49 and filensin contributing to disease, we examined whether the pathology seen in $VimR_{113}C$ lenses was caused by their disruption. CP49 and filensin appeared unaffected when analysed using immunofluorescence microscopy and did not colocalise with vimentin, which suggests that the aggregates do not include the so-called beaded filament proteins and do not disturb the formation of beaded filaments (Fig. 6B-C). Furthermore, immunoblotting demonstrated that changes occur neither in the expression nor in

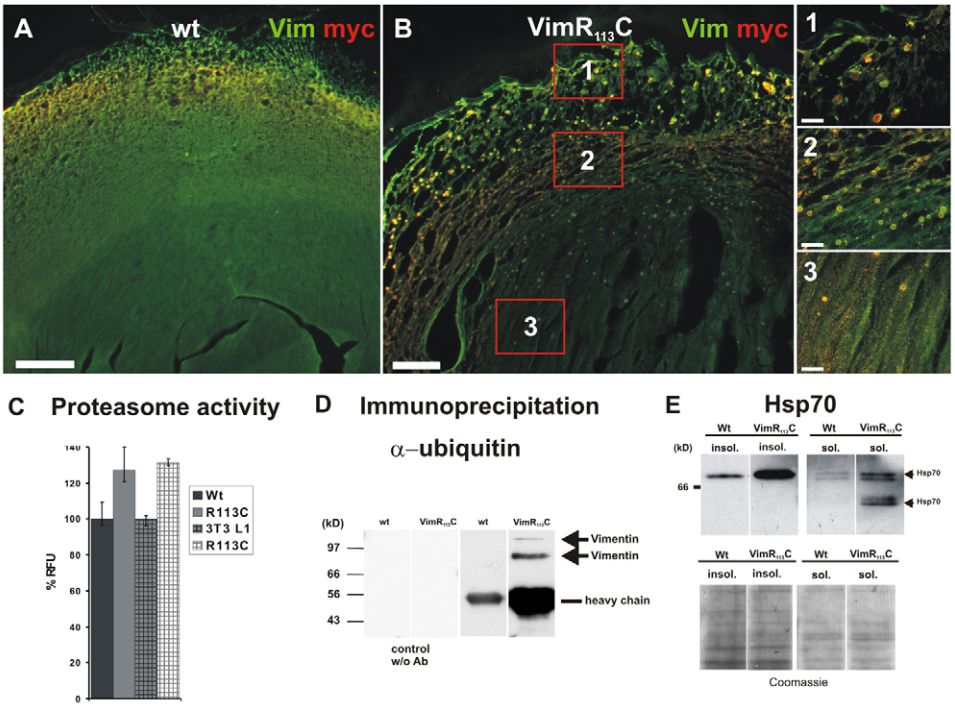

Fig. 5. Increased proteasome activity and reversibility of vimentin aggregates in vivo. (A,B) Immunofluorescence analysis of lenses from 4-month-old $VimR_{113}C$ transgenic and wt mice, stained with antibodies against total (green) and transgenic vimentin (red). Panels 1-3 show higher magnification of lens areas that represent different stages of fibre cell differentiation. Notice that towards the centre of the lens that contains the oldest fibre cells, vimentin aggregates become dissolved, suggesting that they are transient. (C) Fluorescence-based proteasome assay of extracts from lenses and from cells stably transfected with $VimR_{113}C$. In both settings, a 30% increase in proteasome activity in the mutant, compared with the wt, was detected. (D) SDS-PAGE and immunoblotting for ubiquitin of $VimR_{113}C$ and wt lens extracts after immunoprecipitation with a vimentin antibody. Substantially increased ubiquitylation of vimentin was detected in the transgenic lenses (indicated by arrows). The position of the Ig heavy chain is indicated. (E) Immunoblot for Hsp70 in soluble and insoluble lens extracts of wt and $VimR_{113}C$ transgenic mice. In both fractions, Hsp70 expression was upregulated in $VimR_{113}C$ lenses. Scale Bars: 100 μm (A,B), 15 μm (panels 1-3).

the proteolytic processing of both proteins that accompanies lens differentiation (Fig. 6D,E) (Sandilands et al., 1995b).

At the same time, the type-IV IF protein synemin – which is expressed at low levels in the lens and can form heteropolymeric IF with vimentin – was detected in many aggregates (Fig. 7F). In control sections, however, it colocalised with vimentin along the plasma membrane (Fig. 7E) (Granger and Lazarides, 1984; Tawk et al., 2003). This prompted us to investigate the distribution of the cytoskeletal linker protein plectin, which can bind to vimentin, synemin and actin (Wiche, 1998). A C-terminal antibody recognising most plectin isoforms detected an unaltered localisation of plectin at the cell adhesion complex along the lens fibre cortex (Fig. 7C,D) (Straub et al., 2003). This suggests that the interaction between vimentin and synemin is stronger than between plectin and both these proteins. Furthermore, the cortical actin was most similar to control lenses (Fig. 7A,B). Therefore, $VimR_{113}C$ most probably causes structural alterations in the lens by disrupting the endogenous vimentin cytoskeleton, in analogy to dominant mutations in other IF disorders. Future studies will have to address to which extent vimentin, in addition to CP49 and filensin, is necessary for lens integrity.

Effect of mutant vimentin on membrane organisation and cytosolic interactions

To begin to understand how mutant vimentin might cause the structural damage ultimately leading to a lens cataract, we investigated the organisation and distribution of focal adhesions in 3T3L1 fibroblasts stably transfected with $VimR_{113}C$ by immunofluorescence microscopy. Others have recently suggested that synemin localises to focal adhesions in liver stellate cells and may be involved in linking vimentin to these adhesion sites (Uyama et al., 2006). In agreement, a partial colocalisation of vimentin with talin and vinculin was detected at focal contacts in 3T3L1 cells (Fig. 8A,C,E,G) (Tsuruta and Jones, 2003; Uyama et al., 2006). In $VimR_{113}C$-expressing cells, the localisation of talin and vinculin (Fig. 8B,D) and their interaction with β1-integrin (Fig. 8F,H) remained unaltered, whereas their interaction with vimentin was disrupted, as shown by the scattered distribution of vimentin aggregates throughout the cytosol (Fig. 8B,D,F,H, and corresponding insets). We conclude that, although the connection between the vimentin IF network and focal adhesions is disturbed, vimentin aggregates do not influence the distribution and localisation of major components of focal adhesions in cultured cells. It is conceivable that in lens fibre cells, which also express synemin, $VimR_{113}C$ severs the contact with talin- and vinculin-containing junctions and recruits synemin into cytoplasmic aggregates (Fig. 7E,F). This scenario is depicted in Fig. 9, highlighting the interaction of focal adhesions with cellular structures including the cell nucleus through vimentin. We therefore suggest that $VimR_{113}C$ disrupts fibre cell integrity by disrupting vimentin and/or synemin adhesion with membrane attachment sites. Furthermore, mutated vimentin induces upregulation of Hsp70 in vivo, and leads to extensive cytoplasmic aggregates that cause a posterior, age-dependent cataract.

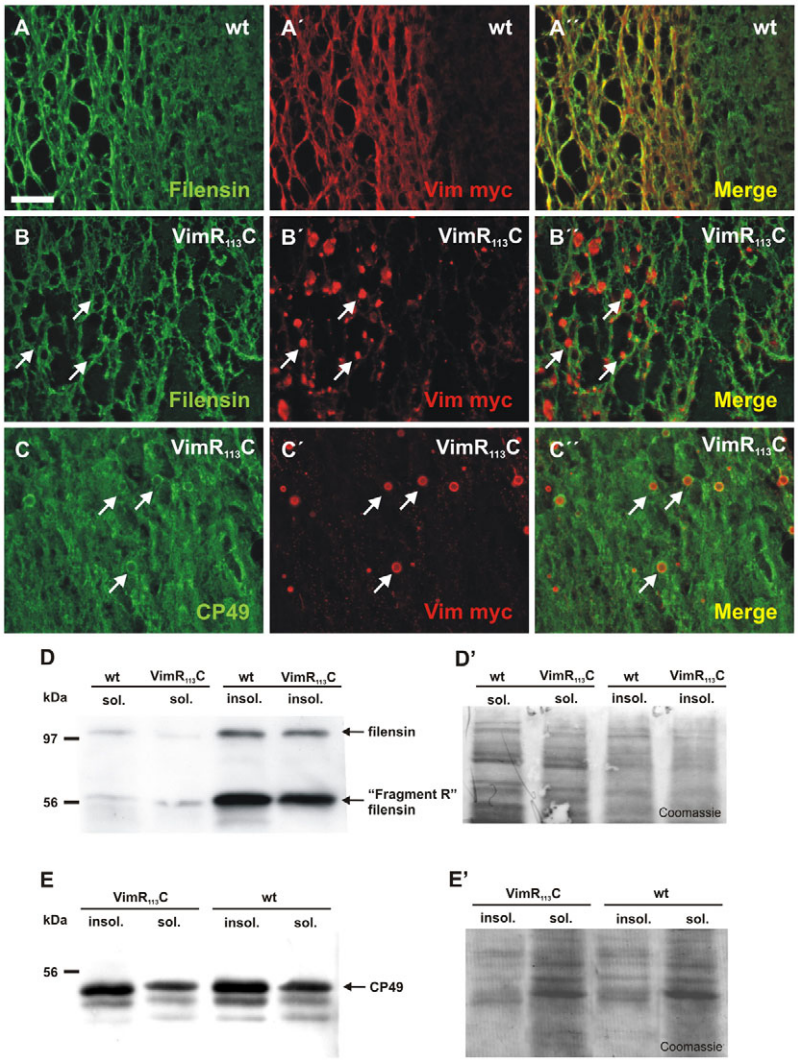

Fig. 6. Unaltered distribution and expression of beaded filaments. (A-C) Immunofluorescence analysis of lens cryosections of 5-month-old $VimR_{113}C$ and wt transgenic mice. Sections were stained using antibodies against filensin, CP49 (both green) and Myc-tagged transgene vimentin (red). Expression and localisation of filensin and mutant vimentin is shown in (A) wt and in (B) $VimR_{113}C$ mice; (C) shows CP49. Merged images document unaltered expression and localisation of major lens proteins in the presence of vimentin aggregates that show no colocalisation. (D,E) Immunoblot detection of filensin and CP49 in soluble (sol.) and insoluble (insol.) lens extracts of wt and $VimR_{113}C$ transgenic mice. (D',E') Similar loadings of the corresponding Coomassie-stained SDS-gels. No changes in the amounts and in the processing of major lens proteins were detected. 'Fragment R' filensin marks a major processing product of filensin, in agreement with previous findings (Sandilands et al., 1995b). Scale bar: 20 μm.

Discussion

Vimentin is widely expressed in all mesenchymally derived cells and both its amino acid sequence and its tissue-specific expression patterns are highly conserved during evolution from primitive fish to humans (Schaffeld et al., 2001). In view of a large number of in vitro and cell culture studies that link it to fundamental processes – including lipid metabolism, intracellular transport, malignant transformation, cell motility and stress response – it is surprising that vimentin has so far not been linked to any specific disease (Herrmann and Aebi, 2004; Colucci-Guyon et al., 1994). Only one study, in which chicken vimentin was more than tenfold overexpressed in the lens of transgenic mice, reported severe lens degeneration (Capetanaki et al., 1989). This phenotype appeared non-specific, as it is highly reminiscent to the ectopic overexpression of other proteins in the lens, for example, the SV40 large T antigen (Gotz et al., 1991).

To investigate vimentin function in vivo, we modified an approach that was first described to identify keratin mutations in EBS and GFAP mutations in Alexander disease (Vassar et al., 1991; Messing et al., 1998; Li et al., 2002). In contrast to other studies, we used the endogenous vimentin promoter, leading to physiological levels of vimentin protein. Thereby, we were able to demonstrate that vimentin has a major function in the eye lens. Despite the accumulation of vimentin aggregates in all mesenchymal cells of the animal, the resulting pathology was restricted to posterior cataracts in lens fibre cells. This rules out that vimentin aggregates per se are generally toxic in mesenchymal tissues. We demonstrate that in lens fibre cells, expression of mutant vimentin causes an increase in Hsp70, which extensively colocalised with mutated vimentin in inclusions. Furthermore, we have shown for the first time that, in contrast to desminopathies and Alexander disease, vimentin-containing aggregates are not terminal but transient structures that ultimately become degraded, even in postmitotic cells (Omary et al., 2004; Li et al., 2002). This activity is in line with findings on the dynamic behaviour of disease-type keratin aggregates in cultured cells but in contrast to certain polyglutamine inclusions (Werner et al., 2004; Kim et al., 2005).

Given that keratin K14 when carrying the $K14R_{125}C$ mutant, which is equivalent to $VimR_{113}C$, becomes ubiquitylated, and that this modification induces phosphorylation of the stress-activated kinase Jun – which in turn can result in an unfolded protein response (Yoneda et al., 2004) – we investigated whether similar pathways are activated in lenticular tissues and in a cell culture model (Schietke et al., 2006; Yoneda et al., 2004). The considerable upregulation of Hsp70 in both settings and the induction of Jun activity in cultured cells (Ruth Schietke and T.M.M., unpublished data) support the notion that dominant IF mutations induce a stress response that is accompanied by an increase in Hsp70 and in proteasome activity by 30%. This is most probably the reason for the degradation of vimentin aggregates observed by us, and might contribute to the overall lens pathology. Since aggregates caused by mutated vimentin do only colocalise with synemin, but not with CP49, filensin or other cytoskeletal proteins examined, they most probably contain predominantly vimentin, synemin and chaperones. Mechanistically, this can be explained by the fact that point-mutated vimentin causes a misfolding of early-assembly complexes, followed by assembly of these misfolded subunits into aggregates. Apparently, these are accessible by proteasomes. Future experiments will have to show whether their degradation involves co-chaperones such as CHIP, as reported previously (Arndt et al., 2007).

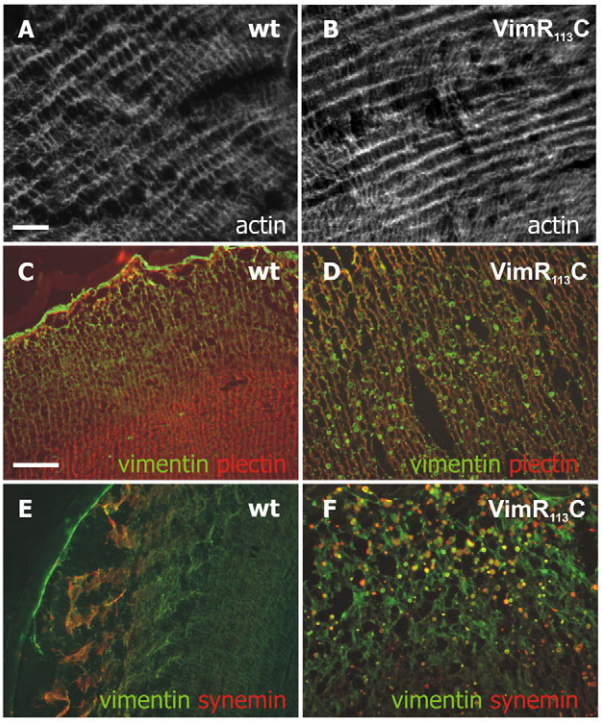

Fig. 7. Distribution of cytoskeletal and vimentin-associated proteins. (A,B) Immunofluorescence analysis of lens cryosections of (A) wt and (B) $VimR_{113}C$ mice. Sections were stained using phalloidin to visualise F-actin. In mutant lenses actin localisation was not altered. (C,D) Double labelling of lens sections showing plectin (red) and vimentin (green). In control sections, both proteins were distributed underneath the plasma membrane. In $VimR_{113}C$ lens sections, the submembraneous localisation of plectin was retained, whereas vimentin formed extensive aggregates. (E,F) Double immunofluorescence showing synemin (red) and vimentin (green). Synemin, which can heteropolymerise with vimentin, was relocalised to some but not all vimentin aggregates, suggesting that the interaction of vimentin and synemin is maintained, whereas their interaction to membrane attachment complexes is severed. Scale bars: 10 µm (A,B), 20 µm (C-F).

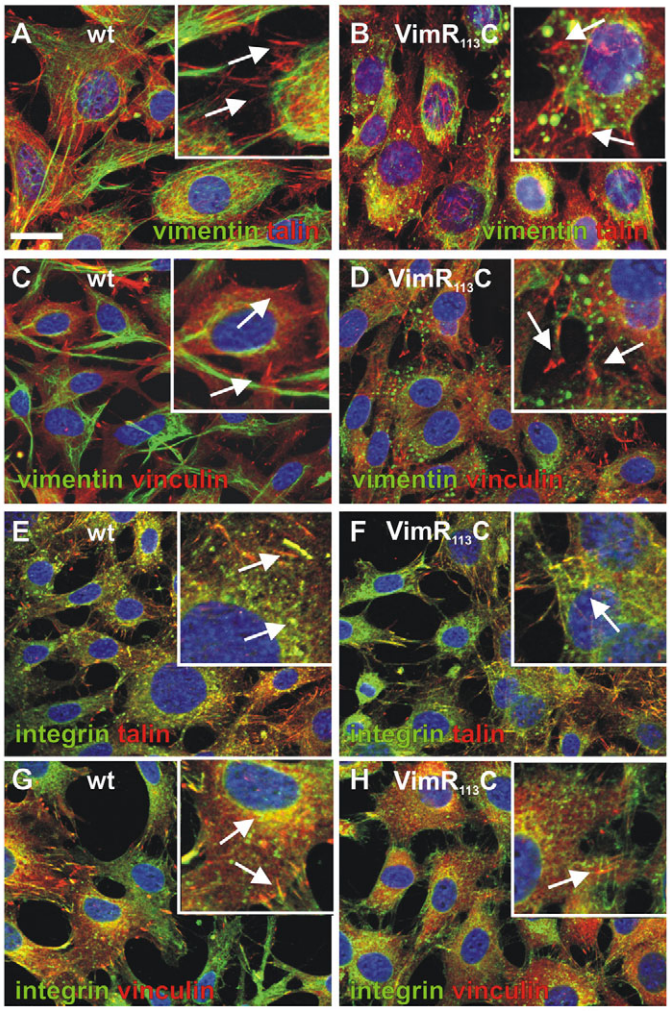

Fig. 8. Normal focal adhesions in fibroblasts expressing $VimR_{113}C$. Double immunofluorescence of focal adhesion proteins in wt and $VimR_{113}C$ 3T3L1 fibroblasts. (A,C) Interaction of vimentin with talin and vinculin at the focal adhesions (arrow in inset). (B,D) Unaltered localisation of talin and vinculin in the presence of cytosolic vimentin aggregates (arrows). (E,G) Colocalisation of vinculin and talin with β1-integrin at focal adhesions. (F,H) Localisation of talin and vinculin at focal adhesions, marked by β1-integrin is unaltered in $VimR_{113}C$-expressing fibroblasts. These data suggest that $VimR_{113}C$-containing IFs are unable to interact stably with focal adhesions. Scale bar: 20 µm.

How can we explain the highly specific pathology linked to the $VimR_{113}C$ mutation in the posterior eye lens given that vimentin is present in the lens epithelium and in differentiated fibre cells? In the former, where vimentin is coexpressed with GFAP, it failed to form aggregates, consistent with its low expression levels, compared with that of GFAP (Hatfield et al., 1984). In support, in vitro co-assembly of wt and mutant vimentin demonstrated that filament formation was abolished in the presence of 50% $VimR_{113}C$, whereas the presence of 10% mutant protein had little influence (Schietke et al., 2006). Furthermore, the turnover of lens epithelial cells, together with the ability of GFAP and vimentin to heteropolymerise, might explain the lack of a detectable defect in the regenerative epithelium.

During lens development and differentiation, vimentin is first localised along the basal region of epithelial and primary fibre cells, before it becomes closely associated with the plasma membrane in extended fibre cells (Blankenship et al., 2001; Sandilands et al., 1995a). This suggests its involvement in the extension process during which fibre cells represent a population of migratory cells. Ultimately, the fibre cell basal membrane zone, which constitutes the posterior aspect of the lens, detaches from the lens capsule and contacts cells from the opposite side of the lens (Bassnett et al., 1999). In fibre cells, two kinds of cell adhesion complex mediate the interaction with the cortical cytoskeleton. The first is formed by N-cadherin and cadherin 11, and is associated with α- and β-catenin, plakoglobin, $p120^{ctn}$ (also known as CTNND1) and vinculin. The second is enriched on the long aspects of fibre cells and comprises ezrin, periplakin, periaxin and desmoyokin, together with plectin, spectrin and moesin (Straub et al., 2003). In contrast to the keratin-desmosome linkage which has been extensively studied and is well defined by disease mutations, very little is known about how vimentin or any of the other IF proteins are attached to adhesion complexes in the lens (Fuchs and Cleveland, 1998; Getsios et al., 2004). In fibroblasts, $p120^{ctn}$ has been suggested to link vimentin to N-cadherin, whereas in endothelial cells plakoglobin and desmoplakin connect vimentin to VE-cadherin (Kim et al., 2005; Kowalczyk et al., 1998; Lampugnani and Dejana, 1997). Given that mutations in desmosomal proteins

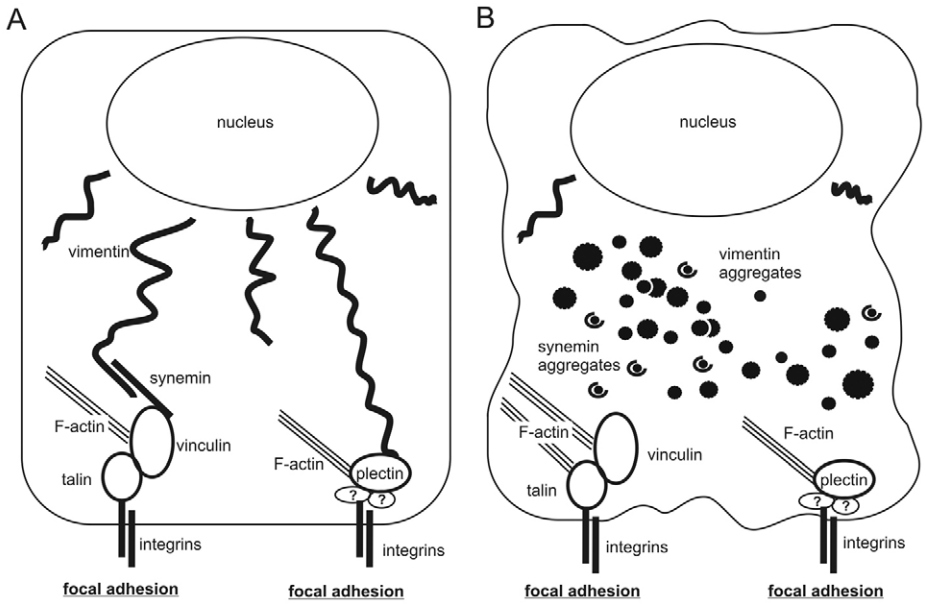

Fig. 9. Model of interaction between vimentin and focal adhesion proteins. (A) In fibroblasts, the vimentin-IF network is connected to integrins through interactions with synemin and vinculin or through plectin. (B) Expression of mutant vimentin in fibroblasts causes aggregate formation and severed connection of IF to focal adhesions. The presence of synemin in vimentin aggregates and the unaltered localisation of vinculin and plectin at focal adhesions suggest a stronger association with vimentin compared with other proteins of the focal adhesion.

and keratins can affect both the integrity of desmosomes and that of the keratin cytoskeleton, we hypothesise that the $VimR_{113}C$ mutation weakens the association with lens-adhesion complexes and ultimately leads to the posterior capsule rupture. This conclusion is supported by the EM analysis of $VimR_{113}C$ lens sections, which demonstrate a highly pleated membrane organisation and a weakened interaction of dorsal fibre cells (Fig. 4). When placed in the context of epidermal keratin disorders, where mechanical stress has a major role, an additional factor may become important to explain the dorsal capsule rupture in $VimR_{113}C$ mice. During lens accommodation, the basal membrane zone is exposed to considerable mechanical forces. Our current model of the interactions between vimentin IF and membrane adhesion sites on the molecular level suggests that the integration of the cytoskeleton with focal adhesions is corrupted because of the collapse of the vimentin IF system and its ability to serve as mechanical 'stress absorber' (see Fig. 9).

What other mechanisms are known to contribute to cataract formation and how do they relate to the phenotype reported in our study? Mutations in genes that encode connexins or crystallins, but also in the IF proteins CP49 and filensin, can cause cataracts (for a review, see Graw, 2004; Perng et al., 2007). Disruption of the gene encoding connexin 46 has been shown to cause increased Ca^{2+} influx, which mediates proteolytic processing of γ-crystallin and leads to its aggregation (Baruch et al., 2001). The mechanism by which CP49 mutants cause a cataract is not known. The analysis of both CP49- and filensin-null mice support the hypothesis that these IF proteins are required to maintain the transparency of the lens (Perng and Quinlan, 2005; Perng et al., 2007). Mutations in both murine and human γ-crystallins can alter their aggregation properties such that they accumulate in the nucleus of primary lens fibre cells and eventually induce cataracts, possibly by the initial depletion of transcription factors, similar to a mechanism postulated for huntington (Sandilands et al., 2002). We found no evidence for an altered differentiation of lens fibre cells in $VimR_{113}C$ mice, making such a mechanism unlikely. The chaperones αA- and αB-crystallin are closely associated with the lens IF cytoskeleton and have been shown to increase the solubility of vimentin in vitro, implying that they may be involved in regulating vimentin reorganisation in vivo (Perng and Quinlan, 2005). In fact, mutations in αB-crystallin cause polar cataracts and a myofibrillar myopathy that is very similar to desmin myopathies, thus supporting an interdependence of IF and αB-crystallin (Graw, 2004; Vicart et al., 1998). We noticed, however, that mutations in αB-crystallin cause polar cataracts, whereas those in $VimR_{113}C$ led to a posterior cataract. Finally, the finding that a dominant vimentin mutation causes a distinct cataract in mice provides a rationale for the mutation analysis of the human vimentin gene in familial cataracts.

Materials and Methods

Mice and genotyping

All experiments were approved by the University of Bonn Health Sciences Animal Welfare Committee and followed the guidelines of the German Council on Animal Care. The different vimentin constructs used have been previously described (Schietke et al., 2006). Transgenic mice were generated at the Karolinska Institut, Center for Transgene Technologies, (Stockholm, Sweden) in a CBA background. Founder animals were backcrossed to C57Bl/6. Mice were analysed and maintained on this background for more than five generations.

Detection of the vimentin transgene was carried out in 25 μl PCR reactions as follows: 20 mM Tris-HCl (pH 8.4), 50 mM KCl, 1.25 mM $MgCl_2$, 250 μM dNTPs, 0.5 μM of both 5′ (5′-CTCATCTCAGAAGAGGATCTG-3′) and 3′ (5′-CTTGAA-CTCAGTGTTGATGGC-3′) primers, 1 unit of *Taq* DNA polymerase and 2 μl (from a total volume of 200 μl) of genomic DNA extracted from mouse tail tips. Temperature profile was: 95°C for 5 minutes, followed by 35 cycles of 95°C for 30 seconds, 55°C for 30 seconds and 72°C for 25 seconds. Subsequently, a final extension step at 72°C for 5 minutes was carried out. Amplification of the transgene resulted in a band of 306 bp.

Protein biochemistry

Total protein extracts were prepared as described previously (Reichelt et al., 1999) and subjected to SDS-PAGE. IF-enriched cytoskeletal extracts were prepared by lysis of lenses for 15 minutes in a homogeniser (Braun, Germany) with ice-cold low-salt buffer (10 mM Tris-HCl pH 7.6, 140 mM NaCl, 5 mM EDTA, 5 mM EGTA, 0.5% Triton X-100, 2 mM phenylmethylsulfonyl fluoride, a subsequent centrifugation step to separate the soluble from the insoluble (cytoskeletal) fraction, which was then resuspended in ice-cold high-salt buffer (10 mM Tris-HCl pH 7.6, 140 mM NaCl, 1.5 M KCl, 5 mM EDTA, 5 mM EGTA, 1% Triton X-100, 2 mM phenylmethylsulfonyl fluoride, homogenised and pelleted by centrifugation (Magin et al., 1998). HRP-conjugated secondary antisera (Dianova, Germany) were diluted 1:30,000. For detection, Super Signal (Pierce) was used. Densitometric measurements were performed using the ImageJ-Program (National Institutes of Health, http://rsb.info.nih.gov/ij/).

Caspase, protease and transglutaminase assays of lens- and cell homogenates

For proteasome analysis, 6 dissected lenses or a confluent cell layer from one 10 cm cell culture dish were homogenized at 4°C for 10 minutes in 2 ml Earle's balanced salt solution (EBSS) using a Potter-Elvehjem homogeniser (Braun, Germany) at 1200 rpm . Cleavage of the synthetic proteasome substrate III (Calbiochem) was measured with a Tecan Genios Spectrafluor Plus multititer plate reader (Tecan, Germany) as described previously (Petersen et al., 2004).

For the caspase assay, six dissected lenses or 5×10^6 cultured cells were homogenised at 4°C in 3 ml ice-cold lysis-buffer (25 mM HEPES pH 7.5, 0.1% Triton X-100, 5 mM $MgCl_2$, 2 mM DTT, 1.3 mM EDTA, 1 mM EGTA) using a Potter-Elvehjem homogeniser at 1200 rpm for 10 minutes. Homogenates were centrifuged at 20,800 ***g*** at 4°C and supernatants were used for the Caspase-Glo 3/7 assay, following the manufacturer's protocol (Promega, Germany). The assay reaction was performed at room temperature for 30 minutes before luminescence signals were detected using a Tecan Genios Spectrafluor Plus plate reader (Tecan, Germany). Each data point represents the average of four wells. A blank control value has been subtracted from each point.

For the transglutaminase assay, lenses were homogenised in 3 ml of 50 mM Tris-HCl (pH 7.5) and 100 mM NaCl using a Potter-Elvehjem homogeniser. The assay was performed as described previously (Clement et al., 1998).

Immunoprecipitation

Protein extracts for immunoprecipitations were prepared by lysis of lenses in a homogeniser (Braun, Germany) in ice-cold RIPA-buffer (25 mM Tris-HCl, pH 7.5, 150 mM NaCl, 1% Nonidet P40, 2 mM EGTA, 2 mM EDTA) supplemented with protease inhibitors (Roche, Germany) for 20 minutes. Homogenates were incubated on ice for an additional 40 minutes and then centrifuged at 20,000 ***g*** for 20 minutes at 4°C. The protein concentration of the supernatant was measured using the Bradford method (Bradford, 1976) and supernatant was incubated with vimentin antibody (4-6 μg) at 4°C for 1 hour while rotating the sample. After addition of 20 μl protein-(A)-Sepharose slurry (Amersham, Germany) solution was incubated at 4°C for 1 hour while rotating the sample. Beads were pelleted and washed five times with RIPA-buffer. Beads were resuspended in Laemmli buffer, heated for 3 minutes at 95°C and proteins were separated by SDS-PAGE. Ubiquitin was detected by incubation with antibodies after blotting on PVDF membranes.

Histology, immunofluorescence and EM of animal tissues

For immunofluorescence microscopy eyes were isolated, mounted in Tissue-Tek (Sakura Finetek, The Netherlands) and immediately frozen in isopentane at –80°C. A Leica CM1900 cryomicrotome was used to cut sections of 5 μm thickness at –21°C. Frozen tissue sections were fixed in acetone at –20°C for 10 minutes and processed for immunofluorescence as described (Reichelt et al., 1997). Sections were examined with a fluorescence photomicroscope (Axiophot 2E; Carl Zeiss, Germany) at room temperature, equipped with Zeiss Plan-Neofluar/Apochromat 63×/1.4 and 40×/1.30 oil immersion, 25×/0.80 multi-immersion, and 10×/0.30 air objective and recorded with a digital camera (AxiocamHR, Carl Zeiss, Germany). Image analysis and processing were performed using the AxionVision LE 4.6 (Carl Zeiss, Germany) and Adobe Photoshop 6.0 software (Adobe Systems). EM was essentially performed as described previously (Reichelt et al., 2001).

Histology was carried out on eyes of 45-week-old mice which were dissected, fixed in 4% formalin (in PBS) over night and embedded in paraffin. Sections (4 μm) were stained with haematoxylin and eosin. Images were recorded with a Nikon 90i microscope, equipped with a Nikon DSRi camera and assembled in Adobe Photoshop.

Antibodies

Primary antibodies were used for immunofluorescences reactions in the following dilutions: GP53 against vimentin (Progen, Germany) 1:100, 9E10 against Myc (Sigma-Aldrich, Germany, Hybridoma) neat, antibody 3241 against filensin 1:50, and antibody 2980 against CP49 1:50 (both kindly provided by Roy Quinlan, Durham University, UK), α-HSP70 (Santa Cruz, Germany) 1:400, phalloidin against actin (Invitrogen, Germany) 1:20, a-Syn against synemin (kindly provided by Denise Paulin, CNRS UMR 7079, Paris, France) 1:200, HD1 against plectin (kindly provided by Katsushi Owaribe, Division of Biological Sciences, Nagoya, Japan) 1:200, 8D4 against talin (Sigma-Aldrich, Germany) 1:250, H-300 against vinculin (Santa Cruz, Germany) 1:400, antibody against β1-integrin (kindly provided by Reinhard Fässler, MPI, Martinsried, Germany) 1:50.

For western blotting the following antibody dilutions were used: P4G7 against ubiquitin (Abcam, UK) 1:1000, GP53 against vimentin (Progen, Germany) 1:2000, antibody 3241 against filensin and antibody 2980 against CP49 both 1:500, α-HSP70 (Santa Cruz, Germany) 1:4000.

Secondary antisera were either Alexa-Fluor-488- or Alexa-Fluor-594-conjugated (Molecular Probes, The Netherlands), IgG1 sub-class-specific Texas-Red-conjugated (Southern Biotech, Birmingham, AL), Cy3- or HRP-conjugated (Dianova, Germany).

Cell lines and cell culture

The cell lines used have been described previously (Schietke et al., 2006). Cells were cultured in DMEM supplemented with 10% FCS (Invitrogen, Germany) and incubated at 37°C and 5% CO_2.

This work was supported by the DFG (Ma 1316/7 and He 1853/5-1). The authors are grateful to Roy Quinlan, Denise Paulin, Reinhard Fässler and Katsushi Owaribe, who provided antibodies. We like to thank Silke Loch and Tanja Wilke for excellent technical assistance and maintaining of mice, Ruth Schietke and Dominique Bröhl for construction of vectors and cell lines and Dieter Hartmann for advice on light microscopy. M.M. is supported by fellowship from the German Research Council (GRK 804).

References

Albers, K. and Fuchs, E. (1987). The expression of mutant epidermal keratin cDNAs transfected in simple epithelial and squamous cell carcinoma lines. *J. Cell Biol.* **105**, 791-806.

Arndt, V., Rogon, C. and Hohfeld, J. (2007). To be, or not to be – molecular chaperones in protein degradation. *Cell. Mol. Life Sci.* **64**, 2525-2541.

Bachmann, S., Kriz, W., Kuhn, C. and Franke, W. W. (1983). Differentiation of cell types in the mammalian kidney by immunofluorescence microscopy using antibodies to intermediate filament proteins and desmoplakins. *Histochemistry* **77**, 365-394.

Bar, H., Mucke, N., Katus, H. A., Aebi, U. and Herrmann, H. (2007). Assembly defects of desmin disease mutants carrying deletions in the alpha-helical rod domain are rescued by wild type protein. *J. Struct. Biol.* **158**, 107-115.

Baruch, A., Greenbaum, D., Levy, E. T., Nielsen, P. A., Gilula, N. B., Kumar, N. M. and Bogyo, M. (2001). Defining a link between gap junction communication, proteolysis, and cataract formation. *J. Biol. Chem.* **276**, 28999-29006.

Bassnett, S., Missey, H. and Vucemilo, I. (1999). Molecular architecture of the lens fiber cell basal membrane complex. *J. Cell Sci.* **112**, 2155-2165.

Blankenship, T. N., Hess, J. F. and FitzGerald, P. G. (2001). Development- and differentiation-dependent reorganization of intermediate filaments in fiber cells. *Invest. Ophthalmol. Vis. Sci.* **42**, 735-742.

Bradford, M. M. (1976). A rapid and sensitive method for the quantitation of microgram quantities of protein utilizing the principle of protein-dye binding. *Anal. Biochem.* **72**, 248-254.

Brehmer, D., Rudiger, S., Gassler, C. S., Klostermeier, D., Packschies, L., Reinstein, J., Mayer, M. P. and Bukau, B. (2001). Tuning of chaperone activity of Hsp70 proteins by modulation of nucleotide exchange. *Nat. Struct. Biol.* **8**, 427-432.

Byun, Y., Chen, F., Chang, R., Trivedi, M., Green, K. J. and Cryns, V. L. (2001). Caspase cleavage of vimentin disrupts intermediate filaments and promotes apoptosis. *Cell Death Differ.* **8**, 443-450.

Capetanaki, Y., Starnes, S. and Smith, S. (1989). Expression of the chicken vimentin gene in transgenic mice: efficient assembly of the avian protein into the cytoskeleton. *Proc. Natl. Acad. Sci. USA* **86**, 4882-4886.

Clement, S., Velasco, P. T., Murthy, S. N., Wilson, J. H., Lukas, T. J., Goldman, R. D. and Lorand, L. (1998). The intermediate filament protein, vimentin, in the lens is a target for cross-linking by transglutaminase. *J. Biol. Chem.* **273**, 7604-7609.

Colucci-Guyon, E., Portier, M. M., Dunia, I., Paulin, D., Pournin, S. and Babinet, C. (1994). Mice lacking vimentin develop and reproduce without an obvious phenotype. *Cell* **79**, 679-694.

Djabali, K., de Nechaud, B., Landon, F. and Portier, M. M. (1997). AlphaB-crystallin interacts with intermediate filaments in response to stress. *J. Cell Sci.* **110**, 2759-2769.

Eshagian, J., Rafferty, N. S. and Goossens, W. (1981). Human cataracta complicata: clinicopathologic correlation. *Ophthalmology* **88**, 155-163.

Franke, W. W., Grund, C., Kuhn, C., Jackson, B. W. and Illmensee, K. (1982). Formation of cytoskeletal elements during mouse embryogenesis. III. Primary mesenchymal cells and the first appearance of vimentin filaments. *Differentiation* **23**, 43-59.

Fuchs, E. and Cleveland, D. W. (1998). A structural scaffolding of intermediate filaments in health and disease. *Science* **279**, 514-519.

Getsios, S., Amargo, E. V., Dusek, R. L., Ishii, K., Sheu, L., Godsel, L. M. and Green, K. J. (2004). Coordinated expression of desmoglein 1 and desmocollin 1 regulates intercellular adhesion. *Differentiation* **72**, 419-433.

Gotz, W., Theuring, F., Favor, J. and Herken, R. (1991). Eye pathology in transgenic mice carrying a MSV-SV 40 large T-construct. *Exp. Eye Res.* **52**, 41-49.

Granger, B. L. and Lazarides, E. (1984). Expression of the intermediate-filament-associated protein synemin in chicken lens cells. *Mol. Cell. Biol.* **4**, 1943-1950.

Graw, J. (2004). Congenital hereditary cataracts. *Int. J. Dev. Biol.* **48**, 1031-1044.

Hatfield, J. S., Skoff, R. P., Maisel, H. and Eng, L. (1984). Glial fibrillary acidic protein is localized in the lens epithelium. *J. Cell Biol.* **98**, 1895-1898.

Herrmann, H. and Aebi, U. (2004). Intermediate filaments: molecular structure, assembly mechanism, and integration into functionally distinct intracellular Scaffolds. *Annu. Rev. Biochem.* **73**, 749-789.

Herrmann, H., Bar, H., Kreplak, L., Strelkov, S. V. and Aebi, U. (2007). Intermediate filaments: from cell architecture to nanomechanics. *Nat. Rev. Mol. Cell. Biol.* **8**, 562-573.

Homan, S. M., Martinez, R., Benware, A. and LaFlamme, S. E. (2002). Regulation of the association of alpha 6 beta 4 with vimentin intermediate filaments in endothelial cells. *Exp. Cell Res.* **281**, 107-114.

Ivaska, J., Pallari, H. M., Nevo, J. and Eriksson, J. E. (2007). Novel functions of vimentin in cell adhesion, migration, and signaling. *Exp. Cell Res.* **313**, 2050-2062.

Kim, S. and Coulombe, P. A. (2007). Intermediate filament scaffolds fulfill mechanical, organizational, and signaling functions in the cytoplasm. *Genes Dev.* **21**, 1581-1597.

Kim, Y. J., Sauer, C., Testa, K., Wahl, J. K., Svoboda, R. A., Johnson, K. R., Wheelock, M. J. and Knudsen, K. A. (2005). Modulating the strength of cadherin adhesion: evidence for a novel adhesion complex. *J. Cell Sci.* **118**, 3883-3894.

Kowalczyk, A. P., Navarro, P., Dejana, E., Bornslaeger, E. A., Green, K. J., Kopp, D. S. and Borgwardt, J. E. (1998). VE-cadherin and desmoplakin are assembled into dermal microvascular endothelial intercellular junctions: a pivotal role for plakoglobin in the recruitment of desmoplakin to intercellular junctions. *J. Cell Sci.* **111**, 3045-3057.

Kreis, S., Schonfeld, H. J., Melchior, C., Steiner, B. and Kieffer, N. (2005). The intermediate filament protein vimentin binds specifically to a recombinant integrin alpha2/beta1 cytoplasmic tail complex and co-localizes with native alpha2/beta1 in endothelial cell focal adhesions. *Exp. Cell Res.* **305**, 110-121.

Lampugnani, M. G. and Dejana, E. (1997). Interendothelial junctions: structure, signalling and functional roles. *Curr. Opin. Cell Biol.* **9**, 674-682.

Li, R., Messing, A., Goldman, J. E. and Brenner, M. (2002). GFAP mutations in Alexander disease. *Int. J. Dev. Neurosci.* **20**, 259-268.

Magin, T. M., Schroder, R., Leitgeb, S., Wanninger, F., Zatloukal, K., Grund, C. and Melton, D. W. (1998). Lessons from keratin 18 knockout mice: formation of novel keratin filaments, secondary loss of keratin 7 and accumulation of liver-specific keratin 8-positive aggregates. *J. Cell Biol.* **140**, 1441-1451.

Magin, T. M., Reichelt, J. and Hatzfeld, M. (2004). Emerging functions: diseases and animal models reshape our view of the cytoskeleton. *Exp. Cell Res.* **301**, 91-102.

Magin, T. M., Vijayaraj, P. and Leube, R. E. (2007). Structural and regulatory functions of keratins. *Exp. Cell Res.* **313**, 2021-2032.

Messing, A., Head, M. W., Galles, K., Galbreath, E. J., Goldman, J. E. and Brenner, M. (1998). Fatal encephalopathy with astrocyte inclusions in GFAP transgenic mice. *Am. J. Pathol.* **152**, 391-398.

Michalczyk, K. and Ziman, M. (2005). Nestin structure and predicted function in cellular cytoskeletal organisation. *Histol. Histopathol.* **20**, 665-671.

Nicholl, I. D. and Quinlan, R. A. (1994). Chaperone activity of alpha-crystallins modulates intermediate filament assembly. *EMBO J.* **13**, 945-953.

Omary, M. B., Coulombe, P. A. and McLean, W. H. (2004). Intermediate filament proteins and their associated diseases. *N. Engl. J. Med.* **351**, 2087-2100.

Perng, M. D. and Quinlan, R. A. (2005). Seeing is believing! The optical properties of the eye lens are dependent upon a functional intermediate filament cytoskeleton. *Exp. Cell Res.* **305**, 1-9.

Perng, M. D., Cairns, L., van den, I. P., Prescott, A., Hutcheson, A. M. and Quinlan, R. A. (1999). Intermediate filament interactions can be altered by HSP27 and alphaB-crystallin. *J. Cell Sci.* **112**, 2099-2112.

Perng, M. D., Sandilands, A., Kuszak, J., Dahm, R., Wegener, A., Prescott, A. R. and Quinlan, R. A. (2004). The intermediate filament systems in the eye lens. *Methods Cell Biol.* **78**, 597-624.

Perng, M. D., Zhang, Q. and Quinlan, R. A. (2007). Insights into the beaded filament of the eye lens. *Exp. Cell Res.* **313**, 2180-2188.

Petersen, A., Zetterberg, M., Sjostrand, J. and Karlsson, J. O. (2004). A new model for assessing proteolysis in the intact mouse lens in organ culture. *Ophthalmic Res.* **36**, 25-30.

Reichelt, J., Bauer, C., Porter, R., Lane, E. and Magin, V. (1997). Out of balance: consequences of a partial keratin 10 knockout. *J. Cell Sci.* **110**, 2175-2186.

Reichelt, J., Doering, T., Schnetz, E., Fartasch, M., Sandhoff, K. and Magin, A. M. (1999). Normal ultrastructure, but altered stratum corneum lipid and protein composition in a mouse model for epidermolytic hyperkeratosis. *J. Invest. Dermatol.* **113**, 329-334.

Reichelt, J., Bussow, H., Grund, C. and Magin, T. M. (2001). Formation of a normal epidermis supported by increased stability of keratins 5 and 14 in keratin 10 null mice. *Mol. Biol. Cell* **12**, 1557-1568.

Robson, R. M., Huiatt, T. W. and Bellin, R. M. (2004). Muscle intermediate filament proteins. *Methods Cell Biol.* **78**, 519-553.

Rothnagel, J. A., Seki, T., Ogo, M., Longley, M. A., Wojcik, S. M., Bundman, D. S., Bickenbach, J. R. and Roop, D. R. (1999). The mouse keratin 6 isoforms are differentially expressed in the hair follicle, footpad, tongue and activated epidermis. *Differentiation* **65**, 119-130.

Sandilands, A., Prescott, A. R., Carter, J. M., Hutcheson, A. M., Quinlan, R. A., Richards, J. and FitzGerald, P. G. (1995a). Vimentin and CP49/filensin form distinct networks in the lens which are independently modulated during lens fibre cell differentiation. *J. Cell Sci.* **108**, 1397-1406.

Sandilands, A., Prescott, A. R., Hutcheson, A. M., Quinlan, R. A., Casselman, J. T. and FitzGerald, P. G. (1995b). Filensin is proteolytically processed during lens fiber cell differentiation by multiple independent pathways. *Eur. J. Cell Biol.* **67**, 238-253.

Sandilands, A., Hutcheson, A. M., Long, H. A., Prescott, A. R., Vrensen, G., Loster, J., Klopp, N., Lutz, R. B., Graw, J., Masaki, S. et al. (2002). Altered aggregation properties of mutant gamma-crystallins cause inherited cataract. *EMBO J.* **21**, 6005-6014.

Schaffeld, M., Herrmann, H., Schultess, J. and Markl, J. (2001). Vimentin and desmin of a cartilaginous fish, the shark Scyliorhinus stellaris: sequence, expression patterns and in vitro assembly. *Eur. J. Cell Biol.* **80**, 692-702.

Schietke, R., Brohl, D., Wedig, T., Mucke, N., Herrmann, H. and Magin, T. M. (2006). Mutations in vimentin disrupt the cytoskeleton in fibroblasts and delay execution of apoptosis. *Eur. J. Cell Biol.* **85**, 1-10.

Straub, B. K., Boda, J., Kuhn, C., Schnoelzer, M., Korf, U., Kempf, T., Spring, H., Hatzfeld, M. and Franke, W. W. (2003). A novel cell-cell junction system: the cortex adhaerens mosaic of lens fiber cells. *J. Cell Sci.* **116**, 4985-4995.

Tawk, M., Titeux, M., Fallet, C., Li, Z., Daumas-Duport, C., Cavalcante, L. A., Paulin, D. and Moura-Neto, V. (2003). Synemin expression in developing normal and pathological human retina and lens. *Exp. Neurol.* **183**, 499-507.

Tsuruta, D. and Jones, J. C. (2003). The vimentin cytoskeleton regulates focal contact size and adhesion of endothelial cells subjected to shear stress. *J. Cell Sci.* **116**, 4977-4984.

Uyama, N., Zhao, L., Van Rossen, E., Hirako, Y., Reynaert, H., Adams, D. H., Xue, Z., Li, Z., Robson, R., Pekny, M. et al. (2006). Hepatic stellate cells express synemin, a protein bridging intermediate filaments to focal adhesions. *Gut* **55**, 1276-1289.

Vassar, R., Coulombe, P. A., Degenstein, L., Albers, K. and Fuchs, E. (1991). Mutant keratin expression in transgenic mice causes marked abnormalities resembling a human genetic skin disease. *Cell* **64**, 365-380.

Vicart, P., Caron, A., Guicheney, P., Li, Z., Prevost, M. C., Faure, A., Chateau, D., Chapon, F., Tome, F., Dupret, J. M. et al. (1998). A missense mutation in the alphaB-crystallin chaperone gene causes a desmin-related myopathy. *Nat. Genet.* **20**, 92-95.

Werner, N. S., Windoffer, R., Strnad, P., Grund, C., Leube, R. E. and Magin, T. M. (2004). Epidermolysis bullosa simplex-type mutations alter the dynamics of the keratin cytoskeleton and reveal a contribution of actin to the transport of keratin subunits. *Mol. Biol. Cell* **15**, 990-1002.

Wiche, G. (1998). Role of plectin in cytoskeleton organization and dynamics. *J. Cell Sci.* **111**, 2477-2486.

Yoneda, K., Furukawa, T., Zheng, Y. J., Momoi, T., Izawa, I., Inagaki, M., Manabe, M. and Inagaki, N. (2004). An autocrine/paracrine loop linking keratin 14 aggregates to tumor necrosis factor alpha-mediated cytotoxicity in a keratinocyte model of epidermolysis bullosa simplex. *J. Biol. Chem.* **279**, 7296-7303.